Internal fibre length concentration in a pressure screen

MARTIN ATKINS, MICHAEL WALMSLEY, ZUBEN WEEDS

Department of Materials & Process Engineering
University of Waikato, New Zealand

ABSTRACT

Localised axial consistency profiles within a pressure screen of a *Pinus Radiata* kraft pulp are reported. Axial Samples were also analysed using a Kajaani FS-200 to obtain fibre length distribution data. Localised consistency in the feed annulus was found to vary considerably and the consistency was found to be less than the feed consistency over some portions of the screen (annular dilution). Changes in consistency along the accept side was fairly constant although subtle changes were observed.

Pulp passage ratios for both the bulk and individual fibre length fractions were calculated using the consistency profiles and fibre length data. In all cases fibre passage decreased along the screen length. Fibre passage was affected by a position effect which is comprised of two factors: flocculation effects, and flow & rotor effects. Fibre fractionation efficiency was found to increase along the length of the screen.

Mechanisms that account for the observed annular dilution, passage ratio and efficiency changes are proposed. These involve flow of both fluid and fibre in the forward and reverse directions across the screen plate, increased flocculation in the feed annulus and the slip velocity between incoming pulp and the rotor tip.

Key Words: Pressure Screening, Fractionation, Fibre Passage, Screening Mechanisms.

INTRODUCTION

Pressure screens play an important part in the manufacture of pulp and paper. They have been utilized predominately to remove contaminants and more recently for the improvement of pulp properties via fibre fractionation. Although numerous fractionation methods have been developed, it is widely accepted that pressure screens are the most practical and economic. As the use of fractionation via pressure screens becomes more widespread the need for versatile and economic systems is expected to increase.

Pressure screens contain highly dynamic and complex flow fields. The rotor in the screen produces a tangential flow along the surface of the screen in addition to generating large pressure variations across the screen. These pressure variations induce flow from the feed annulus to the accept chamber (forward flow) but also periodic flow from the accept chamber to the feed annulus (reverse flow). The purpose of the reverse flow is to unblock the screen apertures that tend to block with fibre and restrict forward flow. The strength, duration, and frequency of the reverse pulse is determined predominantly by the rotor type and rotor speed. Localised pressure variations caused by the rotor have been measured by numerous researchers [1, 2]. These pressure verses time profiles are referred to as pressure pulse signatures and different rotor types produce unique signatures. The pressure pulse signature of the step rotor is shown in Figure 1.

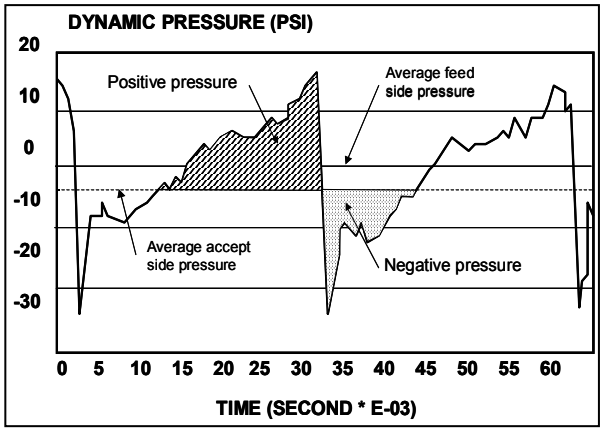

Figure 1 Pressure pulse signature of the Step rotor [1]

Under typical operating conditions the suspension generally increases in consistency within the screen from the feed end to rejects end. This is known as reject thickening and the reject thickening factor (T) is expressed as the ratio of the rejects consistency (C_r) to the feed consistency (C_f) as in Equation 1:

$$T = \frac{C_r}{C_f} \qquad (1)$$

A high reject thickening factor can lead to blocking or plugging of the screen and therefore must be carefully monitored in order to ensure continued operation. The amount of reject thickening that occurs during screening is usually controlled by varying one or both of two factors. The first and most important of these factors is the relative flow rate between the feed (Q_f) and the rejects (Q_r). The ratio of these two flow rates is referred to as the volumetric reject rate (R_v) as in Equation 2. As the volumetric reject rate is lowered reject thickening increases.

$$R_v = \frac{Q_r}{Q_f} \qquad (2)$$

The second factor in controlling reject thickening is the feed consistency. At high feed consistencies the

consistency near the reject end may increase dramatically and cause blocking of the screen.

Passage ratio (P) is used to quantify fibre acceptance through the screen. A number of different ways of expressing passage ratio exist but the most fundamental expression is the ratio of the pulp consistency passing through the aperture which approximates to the accept consistency (C_a) to the pulp consistency on the feed side just up stream from the apertures. This value is somewhere between the feed consistency (C_f) and the reject consistency Cr, depending on the mixing characteristics in the feed side annulus.

For short screens Weeds [3] has shown that an accurate method of calculating passage that is independent of R_v is by dividing the accept consistency by the average consistency in the feed annulus as in Equation 3:

$$P = \frac{C_a}{\frac{C_f + C_r}{2}} \qquad (3)$$

For longer screens a more detailed assessment is required and this is one of the purposes of the work presented in this paper. As the width of the screen section approaches zero the term $(C_f + C_r)/2$ becomes the localised consistency (C_z) as in Equation 4:

$$P = \frac{C_a}{C_z} \qquad (4)$$

Screening and fractionation mechanisms are not well understood at present. Mechanistic understanding must be developed in order to aid both the design of new fractionation systems and optimisation of existing systems [4]. Olson and co-workers have conducted numerous studies into fibre length fractionation caused by slotted and holed apertures [5-8]. These studies, in addition to early fundamental single aperture studies, have demonstrated that fibre length is the dominant fibre property affecting fibre passage, especially at low consistency [9-11]. Furthermore it is also generally accepted that fractionation efficiency increases as the overall thickening factor increases . Consequently it has been assumed that because pulp thickens along the screen length, fractionation efficiency must also increase as the pulp thickens in the screen annulus.

Despite this well established correlation some screen manufacturers have recently partitioned screens, split the accepts into multiple streams and added "deflocculating" and dilution devices into the screen annulus [12]. It is claimed that increased deflocculation in the screen annulus will increase capacity (i.e. increase passage and therefore decrease thickening) which will in turn increase fractionation efficiency. However these claims have not been independently verified and data that has been published to support or justify these claims is far from comprehensive or convincing.

Fibre passage decreases as fibre length increases following a roughly negative exponential curve. Olson *et al.* [6] modelled this relationship using Equation 6 and found that the fitted parameter λ was a useful measure for characterising the relationship between passage and fibre length.

$$P(\ell) = e^{\frac{-\ell}{\lambda}} \qquad (5)$$

Furthermore they found that λ was independent of reject rate and aperture velocity (V_s) for 1mm holes, and suggested that fractionation efficiency can be optimised by operating the screen at a thickening factor greater than two.

Weeds [3] has shown that the relationships between reject thickening, fibre passage and feed consistency are more complex than first thought. As illustrated in Figure 2 he has shown that the rotor type has a strong effect on this relationship and postulated a change in mechanism at different regions of feed consistency. Furthermore it was also demonstrated that screen position had an adverse effect on fibre passage. However the passage of individual fibre length fractions along the screen length has not been studied to date. One advantage of studying the passage of individual length fractions is that the approach elucidates the effect of both fibre length and screen position. Moreover fibre passage and fractionation efficiency can be calculated for each position and length fraction.

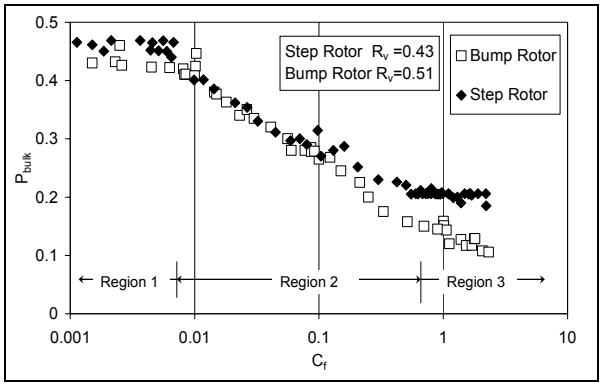

Figure 2 The effect of feed consistency on passage ratio for different rotor types (V_s=0.6m/s, V_t=22m/s) [3]

A study was conducted to elucidate the rate at which reject thickening occurs along the screen length and the passage ratio of different fibre length classes at multiple fixed positions along the screen. Data obtained from consistency measurements and fibre analysis was used to calculate localised fibre passage and fractionation efficiency.

EXPERIMENTAL

Axial consistency profiles were measured using a Beloit MR8 pressure screen which was specifically designed for research purposes. The screen is mounted horizontally and has a tangential feed chamber. The reject stream exits tangentially from the rear of the screen through a 1.5" pipe while the accept stream exits from the centre of the screen housing in a vertical, radial direction. The system is set up on a recycle loop and is fed by a 3000L tank.

The screen basket is 203mm in diameter and 220mm in length. The screen basket used in all these trials had 1mm holes set at a 3mm pitch with an open area of 13.1%. Three rotors were used: a step, bump and foil rotor. A bleached *Pinus Radiata* kraft pulp with an average fibre length of 1.13mm (length-weighted average of 2.28mm) was used.

Localised consistency of the feed annulus and accept chamber was measured using a radial sampling method as illustrated in Figure 3. Localised consistency of the feed annulus was measured by sampling pulp in the annulus using 8mm nominal diameter tubes. The tubes were mounted radially and set flush with the feed side of the screen surface. A total of 10 positions spaced at 20mm intervals along the axial length of the screen were sampled. This allowed a detailed consistency profile in the feed annulus to be measured.

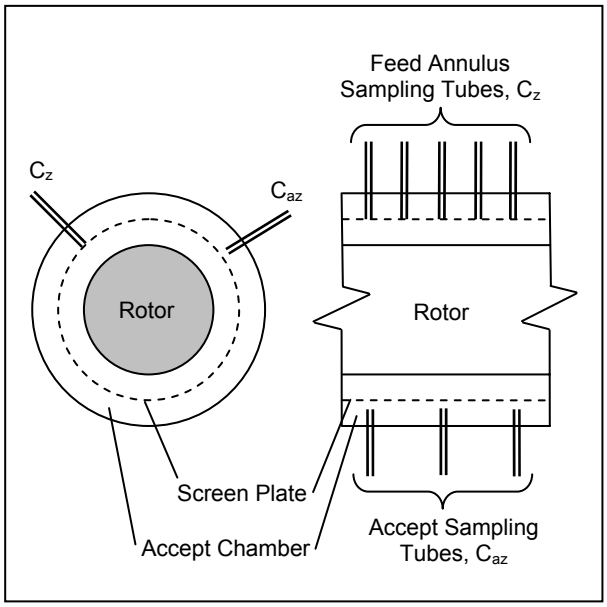

Figure 3 Schematic illustrating radial sampling method of the feed annulus and accept chamber

The localised consistency of the accept chamber was measured by sampling pulp approximately 5mm from the accept side of the screen surface using 8mm nominal diameter tubes. These tubes were also mounted radially and a total of six positions, located at 20, 40, 80, 120, 160 and 180mm along the axial length of the screen, were sampled.

Niinimaki *et al.* [13] used a similar method to measure internal consistency however only one axial position at the centre of the screen was measured. Ämmälä *et al.* [14] and Weeds [3] used both radially mounted tubes as well as an axial method of sampling to measure localised consistency. Weeds found a significant difference in measurement between the two methods however a comprehensive comparison was outside the scope of that study. The authors have since undertaken an extensive comparison of the two methods and have found the radial method to be far more accurate than the axial method.

Axial consistency was measured at two feed consistencies, one corresponding to Region 2 and also Region 3 of the passage vs. feed consistency plot shown in Figure 2. The feed consistency for Region 2 was ≈ 0.15% and for Region 3 ≈ 1%. The accept flow rate was set constant to give a desired average aperture velocity and the reject rate was varied. The range of volumetric reject rates tested varied from between 0.1 and 0.6 except for the higher feed consistency where the lowest reject rate attainable was approximately 0.3 due to screen blocking.

The localised axial consistency of both the feed annulus (C_z) and the accept chamber (C_{az}) was normalised by the feed consistency (C_f) and plotted against screen length (L_z). The normalised consistency of the feed annulus can be considered as the local thickening factor at that axial position.

Fibre length analysis was performed on samples for selected conditions using a Kajaani FS-200. The FS-200 measures the total number of fibres contained in the sample for each 0.05mm length class up to a maximum of 7.2mm. To aid in the analysis these length classes were then grouped into six length fractions based on a modified particle size model. Fibre consistency for each length fraction (C_{nx}) was expressed as the number of fibres per unit volume of suspension. The passage ratio for each fibre length fraction (P_{nx}) was calculated by taking the ratio of the consistency of the fibre length fraction in the accepts ($C_{nx.a}$) and the consistency of the fibre length fraction in the feed annulus ($C_{nx.z}$) as in Equation 7:

$$P_{nx} = \frac{C_{nx.a}}{C_{nx.z}} \qquad (7)$$

In addition to the six length fractions the fibres were also divided into a short and long fibre fraction to examine length fractionation. The short fibre fraction included all length classes up to 2mm and the long fibre fraction from 2mm to 7.2mm. The passage of the short (P_S) and long (P_L) fibre fractions were calculated using Equations 8 & 9:

$$P_S = \frac{C_{S.a}}{C_{S.z}} \quad \text{Short Fibre (8)}$$

$$P_L = \frac{C_{L.a}}{C_{L.z}} \quad \text{Long Fibre (9)}$$

Axial variations in fractionation efficiency were expressed using the separation ratio (α) because other commonly used measures of fractionation efficiency use reject rate as part of the calculation. The separation ratio is expressed in Equation 10:

$$\alpha = 1 - \frac{P_L}{P_S} \qquad (10)$$

For comparison the fractionation index (Φ) was used to express the overall fraction efficiency. The fractionation index is expressed in Equation 11:

$$\Phi = R_v^{P_L} - R_v^{P_S} \qquad (11)$$

The fractionation index is a useful measure as it aims to incorporate the mass flow of short and long fibre to the accept and reject streams. It penalises the rejection of short fibre to the reject stream and the acceptance of long fibre into the accept stream [8]. Therefore a "perfect" fractionation device would separate all short fibre from the long fibre and would have a fractionation index equal to one.

RESULTS AND DISCUSSION

As shown in the passage versus consistency plot in Figure 2, a complex relationship exists between fibre passage ratio and consistency. A consistency in Region 2 was chosen for the first set of experiments (C_f≈0.15%) and axial consistency was measured for a given V_s with reject rate being varied from 0.1 to 0.6. The axial consistency profiles for the step rotor at different reject rates are shown in Figure 4.

It is clear that the overall thickening factor (the last data point on the graph, i.e. L_z=220) increases as the reject rate was decreased. However, as is clearly observed in Figure 4, the axial consistency fell below the feed consistency (i.e. C_z<C_f) thus yielding a localised thickening factor of less than one. This annular dilution in some cases caused the localised consistency in the front half of the screen to reach as low as 70% of the feed consistency. This phenomenon has not previously been reported in the literature. Although it is evident that the overall thickening factor was dependant on the reject ratio, the actual thickening only occurred over the latter part of the screen. The axial dilution occurred despite changing the reject rate and appears to be more severe as the reject rate is increased.

The axial consistency profiles of the bump and foil rotors are also measured at similar operating conditions although the profiles are not given here. The rotor type had a clear effect on the consistency profile, with the bump rotor giving somewhat less annular dilution than the step rotor, while no annular dilution occurred with the foil rotor. This is most likely due to the foil rotor being an open type rotor with substantially different macro flow patterns in the feed annulus than a closed type rotor.

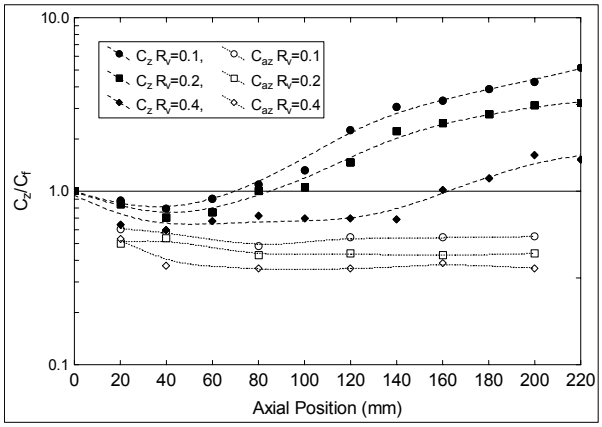

Figure 4 Normalised axial consistency profiles for the Step rotor at a range of reject rates (V_s=0.6m/s, C_f=0.14%, V_t=28m/s)

The rotor tip speed was varied to determine the effect on the axial consistency profile. The axial consistency profile for the step rotor at two different tip speeds are shown in Figure 5. A decrease in tip speed from 28m/s to 17m/s caused the overall thickening factor to increase, the overall passage ratio to decrease and the axial consistency profile to shift up slightly. Furthermore less axial dilution occurred at the lower tip speed.

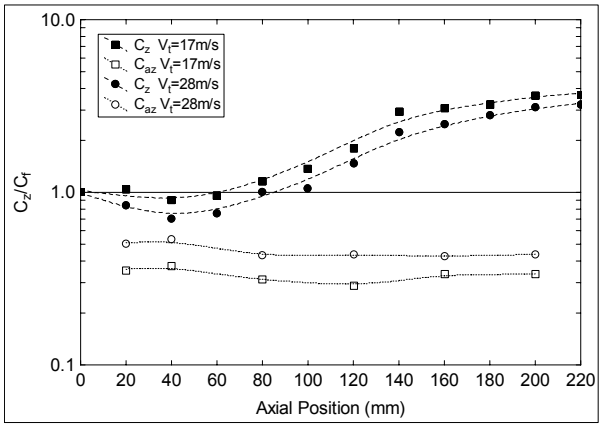

Figure 5 Normalised axial consistency profiles for the Step rotor at R_v=0.2 for two different rotor speeds (V_s=0.3m/s, C_f=0.16%)

Axial consistency profiles were also measured for a feed consistency in Region 3 (C_f≈1%) with operating parameters set to match those used for Region 2. It was found that the axial consistency profiles were

similar in shape to those in Region 2 except that the overall thickening factors were different.

The phenomenon of feed annulus dilution is an interesting discovery and can reasonably be accounted for by only one explanation. If the entire screen is considered, pulp thickens because the accept consistency is lower than the feed consistency. Furthermore the forward flow across the screen is much greater than the reverse flow which gives a positive net flow across the screen. There are limited cases where accept thickening has been reported but this only occurs under very unique and isolated conditions [15]. Accept thickening is where the accept consistency is greater than the feed, the reject consistency is lower than the feed, and a positive net flow across the screen still occurs.

Localised accept thickening is one possible explanation for the phenomenon of annular dilution however it is discounted here as the cause. There was no thickening measured on the accept side of the screen and local accept consistency was fairly constant along the entire length of the screen. Furthermore the conditions used in these trials are well away from those which cause accept thickening.

The most likely explanation is that over the first section of the screen the amount of reverse flow exceeds that of the forward flow thus giving a negative net flow over that section of the screen. It is expected that water and at least the fines would pass in the reverse direction. The suspension coming back in the reverse direction would have a consistency many times less than the feed consistency and would therefore dilute the stock in the feed annulus. At some point along the screen the amount of forward flow would become greater than the reverse flow and cause pulp to thicken. In order to compensate for this section of bulk reverse flow, the flow over the remainder of the screen would be much greater than originally thought.

Another important inference that follows on from this hypothesis is that in order to get the level of dilution in the feed chamber there must be substantially different flow patterns in the accept chamber than is currently expected. Further work is currently being undertaken to experimentally verify the theory of bulk negative flow over a portion of the screen.

Typical passage versus screen length plots for the step rotor at various reject rates are shown in Figure 6. Localised passage ratio of the pulp was calculated using Equation 7. The bulk passage ratio, calculated using Equation 3, is also indicated on the plot. Passage ratio decreased along the length of screen in all cases tested. This is consistent with the findings of Weeds [3] who found that passage ratio decreased along the screen length as a narrow screen section was moved toward the rear of the screen. Despite the bump and step rotors having similar bulk passage ratios the passage at the front of the screen was considerable lower for the bump rotor than the step. This may be because the step rotor has a much larger and longer reverse pulse which in turn gives larger amounts of reverse flow especially at the front of the screen.

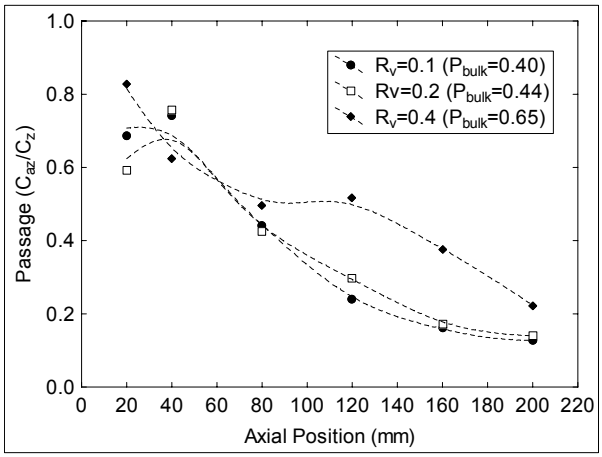

Figure 6 Localised passage ratio changes along the screen length for the for the Step rotor at a range of reject rates (V_s=0.6m/s, C_f=0.14%, V_t=28m/s)

The localised passage ratio also decreased at all positions along the screen length as the rotor speed was decreased from 28m/s to 17m/s as shown in Figure 7. There was a large difference in the bulk passage between the two rotor speeds which was unexpected as the thickening factors were very close to each other.

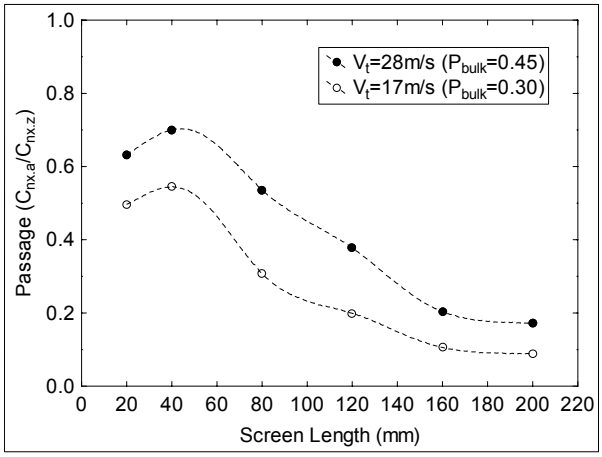

Figure 7 Localised passage ratio changes along the screen length for the for the Step rotor at R_v=0.2 for two different rotor speeds (V_s=0.3m/s, C_f=0.16%)

The passage ratio for each fibre length fraction at different axial positions was calculated using Equation 8 and data obtained from the fibre length analysis. Typical values are shown in Figure 8 for the step rotor at C_f=1.03% and R_v=0.3. Similar trends occurred with both the bump and the foil rotors at both feed consistencies. As is consistent with all previous studies, passage decreased as fibre length increased, but also decreased as the axial position shifted toward

the rear of the screen. Usually only the overall curve (P vs. fibre length) is reported and used as an indication of fractionation efficiency. The decrease in passage along the screen length for each length fraction is also consistent with the trends of decreasing overall passage shown in Figure 6, and Figure 7.

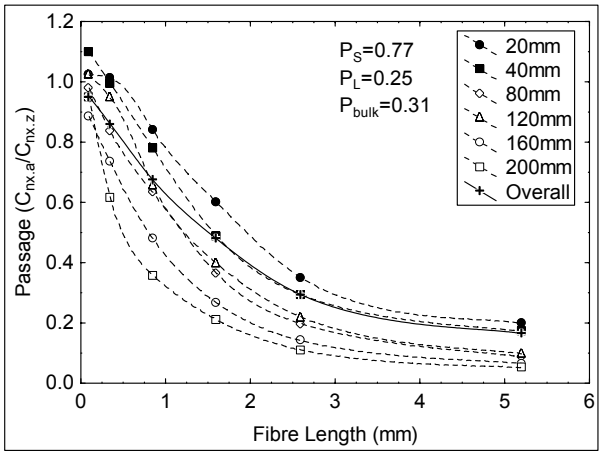

Figure 8 Passage Ratio of individual fibre length fractions at axial locations along the screen length for the Step rotor at R_v=0.3 (V_s=0.6m/s, C_f=1.03%, V_t=28m/s)

The fines have a passage approximately equal to one along the entire length of the screen while for the other length classes the passage is higher at the front of the screen compared to the back. This is expected as the same trend occurred for the bulk passage. As fibre length is the dominant fibre property affecting passage, the passage decreases as the fibre length increases. However as shown in Figure 8 there is also a position effect which also has a major effect on the fibre passage.

The decrease in the passage ratio along the screen length is due to a position effect which is comprised of two factors: a) changes in the suspension properties (flocculation effects) and b) changes in the flow conditions (flow & rotor effects). Weeds [3] has shown using narrow screen sections that bulk passage of a narrow section decreased as the section was moved toward the rear of the screen. He also discounted an entry effect as the cause of the reduction by reversing the axial direction through the screen (i.e. made the rejects end the feed end and visa versa). The same decrease in passage was found. One of the limitations of using narrow screen sections is that the trends may not generalise to a full-length screen. However in light of the data presented here it seems that the trend of decreasing passage along the screen length does apply for a full-length screen.

The parameter λ was calculated for each passage vs. fibre length curve shown in Figure 8 and plotted as a function of screen length in Figure 9. Also shown in Figure 9 is the change in λ for C_f=0.14%. It is evident that for the first part of the screen that λ was much greater at the lower consistency. This is because the passage of the long fibre was much greater over the initial part of the screen as will be illustrated later.

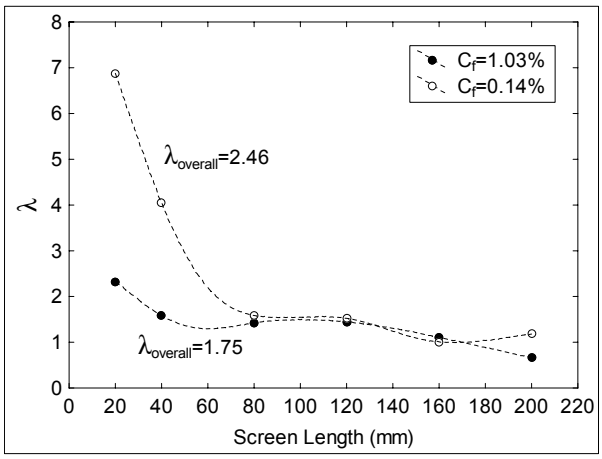

Figure 9 Change in parameter λ along the screen length Step rotor, C_f=0.14% at R_v=0.2 and C_f=1.03% at R_v=0.3 (V_s=0.6m/s, V_t=28m/s)

As a consequence of the difference in passage ratio for the separate length fractions, long fibre will become concentrated in the feed annulus as the suspension progresses along the screen. This will in turn alter the average fibre length of the suspension. Figure 10 shows the localised average fibre length (length weighted average) for the entire screen length of the feed annulus and accepts chamber. The average fibre length of the bulk accepts for both feed consistencies are shown by a horizontal line. The average fibre length of the bulk accepts is the value most often reported in the literature for indicating changes in fibre length due to fractionation. As is seen in Figure 10 there is a variation in the local fibre length in the accept chamber.

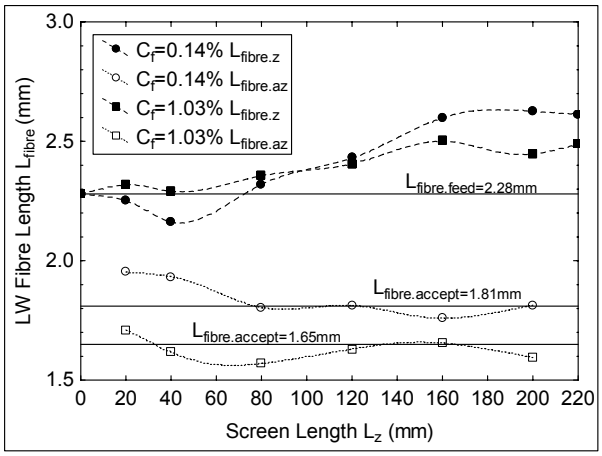

Figure 10 Average fibre length changes along the screen length for the Step rotor, C_f=0.14% at R_v=0.2 and C_f=1.03% at R_v=0.3 (V_s=0.6m/s, V_t=28m/s)

As the suspension travels in the axial direction, long fibre tends to become more concentrated. This increases the average fibre length and coupled with an

increase in consistency, due to thickening, alters the suspension properties and rheology. It is well known that for the same flow conditions and consistency, an increase in average fibre length promotes the tendency for fibres to mechanically entangle and form flocs. Properties such as floc size, floc density, rupture strength, and disruptive shear stress would all be expected to increase with increased fibre length. Increased flocculation has a negative influence on fibre passage, although it may also have a positive impact on fractionation. As fibre length and consistency increase, longer fibre will more likely become mechanically entangled, less likely to be freed from the peripheral of the floc and therefore more readily rejected. Even at lower consistency, such as those used for single aperture studies, long fibre has a much lower passage than short fibre.

The passage ratios of the short and long fibre fractions are useful to illustrate the marked difference in passage between these two fractions. The passage ratio was calculated using Equations 9 & 10. As expected the short fibre had a much higher passage than the long fibre and the passage of both fractions decreased along the screen length as shown in Figure 11. When the feed consistency was increased into Region 3 the passage of the short fibre was similar to that of Region 2 while the passage of the long fibre fraction remained much lower than in Region 2 and also remained relatively unchanged over approximately 70% of the screen length. The much lower passage of the long fibre is thought to be the cause of the large difference in the overall passage of the long fibre for the two feed consistencies. A change in tip speed from 28m/s to 17m/s affected the passage of the long fraction much more than the short fraction (data not presented here). The overall passage of the short fraction was unchanged however the long fraction had a large decrease in passage as the tip speed was altered.

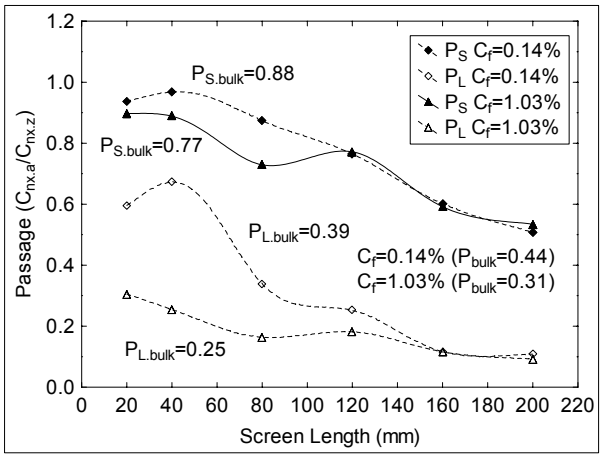

Figure 11 Passage Ratio for Step rotor for the long and short fibre length fractions, C_f=0.14% at R_v=0.2 and C_f=1.03% at R_v=0.3 (V_s=0.6m/s, V_t=28m/s)

The passage of the long and short fibre fractions were used to calculate the separation ratio using Equation 11 and the overall fractionation index using Equation 12. The separation ratio increased along the length of the screen for both feed consistencies as shown in Figure 12, although the change was much less for Region 3.

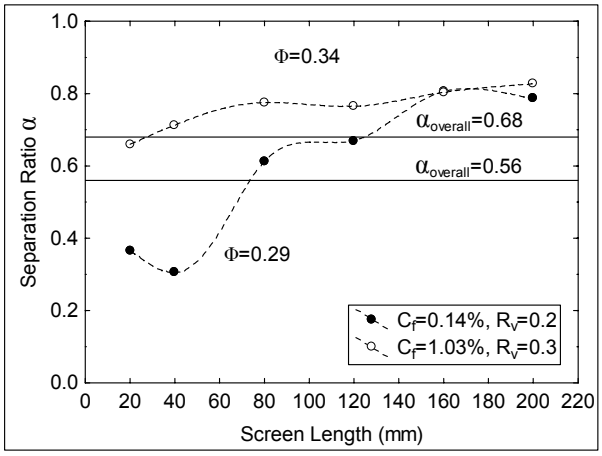

Figure 12 Separation ratio changes along the screen length for the Step rotor, C_f=0.14% at R_v=0.2 and C_f=1.03% at R_v=0.3 (V_s=0.6m/s, C_f=1.03%, V_t=28m/s)

Decreasing the rotor speed caused the separation ratio to increase at all positions along the screen length as shown in Figure 13. The fractionation index also increased from 0.27 to 0.43 as the rotor speed was decreased. This is a significant increase and it must also be noted that there was only a very small increase in the thickening factor when the rotor speed was decreased.

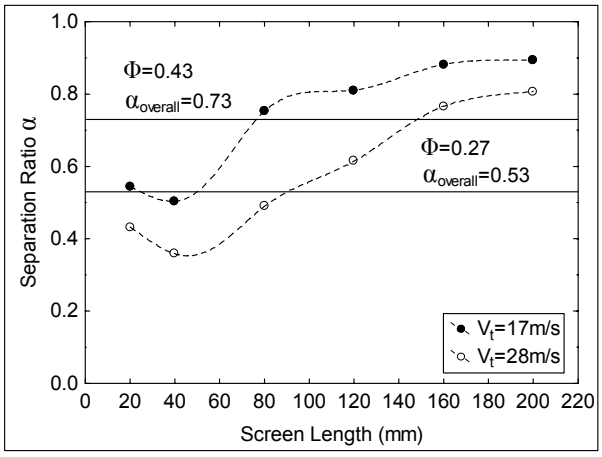

Figure 13 Separation ratio changes along the screen length for the Step rotor at R_v=0.2 for two different rotor speeds (V_s=0.3m/s, C_f=0.16%)

As the stock enters the feed chamber it has an average tangential velocity, V_{tan}, which is much less than the tip speed of the rotor, V_t. When the stock contacts the rotor it will accelerate due to the difference in the velocities. The stock will continue to accelerate as it travels along the screen until at some point along the screen it reaches a maximum V_{tan}. The ratio of V_{tan} to V_t is called the slip factor. The bulk tangential velocity in the annulus has estimated to be about 15% of the tip

speed; however this value has yet to be experimentally verified. This value is taken from single aperture studies that do not use a rotor and therefore may not equal actual values found in a pressure screen. It is also very likely that rotor geometry and the size of the annular gap will affect the slip factor. Tangential velocity profiles measured across an annulus with a rotating cylindrical rotor have shown that the average velocity over approximately 90% of the annular gap to be about 50% of the rotor tip speed [16].

Changing the tangential velocity will have a number of effects on the local behaviour of the screen. The level and intensity of the turbulence will be altered. This is turn will affect the flocculation and rheological properties of the suspension. Flocs readily form in decaying turbulence and can form in an extremely short time. Moreover changes in the tangential velocity will also affect the flow field at individual apertures. It has been shown that the flow field has a great influence on the passage of the fibre through the aperture. In order to maximise fractionation the passage of long fibre should be minimised. As seen in Figure 11, the passage of long fibre and also the short fibre fraction decreases significantly toward the rear of the screen.

CONCLUSIONS

The following conclusions can be drawn from this investigation:

- The axial consistency is variable along the screen length and may be less than the feed consistency (annular dilution) over a portion of the screen.
- The overall passage ratio of the pulp and also the individual fibre length fractions decreased along the screen length for all the rotors and feed consistencies investigated.
- The decrease in the passage ratio along the screen length is due to a position effect which is comprised of two factors: a) changes in the suspension properties (flocculation effects) and b) changes in the flow conditions (flow & rotor effects).
- Long fibre became concentrated in the feed annulus which in turn caused the average fibre length to increase. The average fibre length along the screen length in the accept chamber was fairly constant.
- Varying the rotor speed significantly altered the passage of the long fibre fraction along the screen length which in turn affected the fractionation efficiency.

REFERENCES

1. Yu, C.J. *Pulsation Measurement in a Screen Part 1: Pulse Signature and Magnitude of S-Shape Rotor*. in *Tappi Engineering Conference*. 1994.
2. Pinon, V., Gooding, R.W., & Olson, J.A., Tappi Journal, **2**(10): p. 9-12 2003.
3. Weeds, Z. & Walmsley, M. *Flow and Consistency Variations in Pressure Screen*. in *56th Appita Annual Conference*. Rotorua, New Zealand. 2002.
4. Gooding, R.W., Kerekes, R.J., & Salcudean, M. *The Flow Resistance of Slotted Apertures in Pulp Screens*. in *Fundamental Research Symposium*. Oxford, England. 2001.
5. Olson, J.A. & Wherrett, G., Journal of Pulp and Paper Science, **24**(12): p. 398-403 1998.
6. Olson, J.A., Allison, B.J., & Roberts, N., Journal of Pulp and Paper Science, **26**(1): p. 12-16 2000.
7. Olson, J.A. & Kerekes, R.J., Appita, **51**(2): p. 122-126 1998.
8. Olson, J.A., Journal of Pulp and Paper Science, **27**(8): p. 255-261 2001.
9. Gooding, R.W., *The Passage of Fibres Through Slot in Pulp Screening*, in *Department of Chemical Engineering*. University of British Columbia: Vancouver, Canada 1986.
10. Kumar, A., *Passage of Fibres Through Screen Apertures*, in *Department of Chemical Engineering*. University of British Columbia: Vancouver, Canada 1991.
11. Olson, J.A., *The Effect of Fibre Length on Passage Through Narrow Apertures*, in *Department of Chemical Engineering*. University of British Columbia: Vancouver, Canada. p. 128 1996.
12. Serres, A. & Rees, B., Appita, **55**(4): p. 267-271 2002.
13. Niinimaki, J., Dahl, O., Hautala, J., Tirri, T., & Kuopanportti, H., Tappi Journal, **79**(11): p. 119-123 1996.
14. Ammala, A., Dahl, O., Kuopanportti, H., & Niinimaki, J., Paperi ja Puu, **81**(3): p. 210-215 1999.
15. LeBlanc, P.E. *A Breakthrough in Pressure Screening*. in *Tappi Pulping Conference*. 1986.
16. Antures, J., Axisa, F., & Grunenwald, T., Journal of Fluids and Structures, (10): p. 893-918 1996.

ACKNOWLEDGEMENTS

The authors would like to acknowledge Toby O'Reilly for his assistance. The financial support of the University of Waikato is gratefully acknowledged.